



## Synthesis of pure and mixed Nickel-Cobalt ferrites ( $\text{Ni}_{1-x}\text{Co}_x\text{Fe}_2\text{O}_4$ ) by combustion method and characterization

Ajaypal Singh<sup>a</sup>, Jashanpreet Singh<sup>b</sup> and H. S. Dosanjh<sup>a\*</sup>

<sup>a</sup>Department of Chemistry, Lovely Professional University, Phagwara Punjab, India

<sup>b</sup>Department of Chemistry, Guru Nanak Dev University, Amritsar, Punjab, India

### ABSTRACT

In the present work, synthesis of pure and mixed Nickel-Cobalt spinel ferrite samples,  $\text{Ni}_{1-x}\text{Co}_x\text{Fe}_2\text{O}_4$  ( $x=0, 0.1, 0.3, 0.5$ ), has been carried out with varying composition of Co as substituent. Solution combustion method has been employed for the synthesis of ferrites. For the combustion synthesis oxalic dihydrazide (ODH) was used as a fuel. Various techniques i.e. Fourier transform infrared spectroscopy (FT-IR), X-ray powder diffraction (XRD) and Mössbauer spectroscopy have been used to characterize ferrite samples. Magnetic studies have been carried out by using Vibrating sample magnetometer (VSM). Cobalt substituted ferrites show variation in magnetic properties than pure nickel ferrite. These variations could be explained using the magneto crystalline anisotropy constant, magnetic moment and cation distribution in ferrites. Combustion method leads to the formation of single phase spinel ferrites. Ferrites are also prepared at lower temperature and in shorter time.

**Keywords:** Combustion synthesis, Nanoferrites, Magnetic studies, Mössbauer spectroscopy

### INTRODUCTION

Nano-scale ferrite materials find applications as ferrimagnetic materials in various fields owing to their electrical and magnetic properties [1-3]. Nickel ferrite,  $\text{NiFe}_2\text{O}_4$ , is a soft ferrite while cobalt ferrite,  $\text{CoFe}_2\text{O}_4$ , is a hard ferrite (based on coercivity of the material). As per different nature of these materials, these ferrites are extensively used in various applications [4-8]. Properties of these materials, which are dependent upon microstructure and composition, are also sensitive towards the processing techniques. Various techniques have been employed in the recent years like co-precipitation method [9, 10], sol-gel [11, 12], hydrothermal [13], precursor method [14, 15] and combustion technique [16-18]. Mixed Ni-Co ferrites have been studied recently for their magnetostrictive, structural and magnetic properties [19-21]. Synthesis of nano-scale ferrite materials are considerably the area of recent research as nano-ferrites have potential applications as catalysis [22], gas sensors [23, 24], magnetic drug delivery [25] and dye adsorbent [26-28]. In the present study, solution combustion method has been employed for the preparation of ferrite materials and various physico-chemical techniques are used for characterization.

### EXPERIMENTAL SECTION

Cobalt substituted nickel ferrites having composition  $\text{Ni}_{1-x}\text{Co}_x\text{Fe}_2\text{O}_4$  (where  $x=0, 0.1, 0.3, 0.5$ ) were synthesized by mixing stoichiometric aqueous solutions of nickel nitrate  $\{[\text{Ni}(\text{NO}_3)_2] \cdot 6\text{H}_2\text{O}\}$ , cobalt nitrate  $\{[\text{Co}(\text{NO}_3)_2] \cdot 6\text{H}_2\text{O}\}$  and ferric nitrate  $\{[\text{Fe}(\text{NO}_3)_3] \cdot 9\text{H}_2\text{O}\}$  with oxalic dihydrazide (ODH). Reaction mixture was first concentrated on water bath for 2 hours and then combusted in a muffle furnace at  $600^\circ\text{C}$  for 3 hours which produced fine ferrite powder.

Infra-red studies were carried out by using FTIR-8400S Shimadzu spectrometer. X-ray powder diffraction studies have been carried out by using PANALYTICAL PW3064 X-ray diffractometer with Cu K $\alpha$  source,  $\lambda=1.54 \text{ \AA}$ . Mössbauer spectra of these ferrites have been recorded at 298K by using MB-500 Mössbauer spectrometer with  $^{57}\text{Co}$   $\lambda$ -ray source of 25 mCi embedded in Rhodium matrix and results were fitted using WinNormos. The isomer shift values have been reported with respect to pure iron absorber. Magnetic studies were recorded at room temperature by using vibrating sample magnetometer (VSM- Microsense Instruments).

## RESULTS AND DISCUSSION

The FTIR spectrum of ferrite sample ( $x=0.3$ ) (Fig. 1) show two distinct absorption bands in the range of  $600 \text{ cm}^{-1}$  to  $380 \text{ cm}^{-1}$ . These bands are assigned to tetrahedral (high frequency) and octahedral (low frequency) sites respectively in a spinel structure [29, 30].

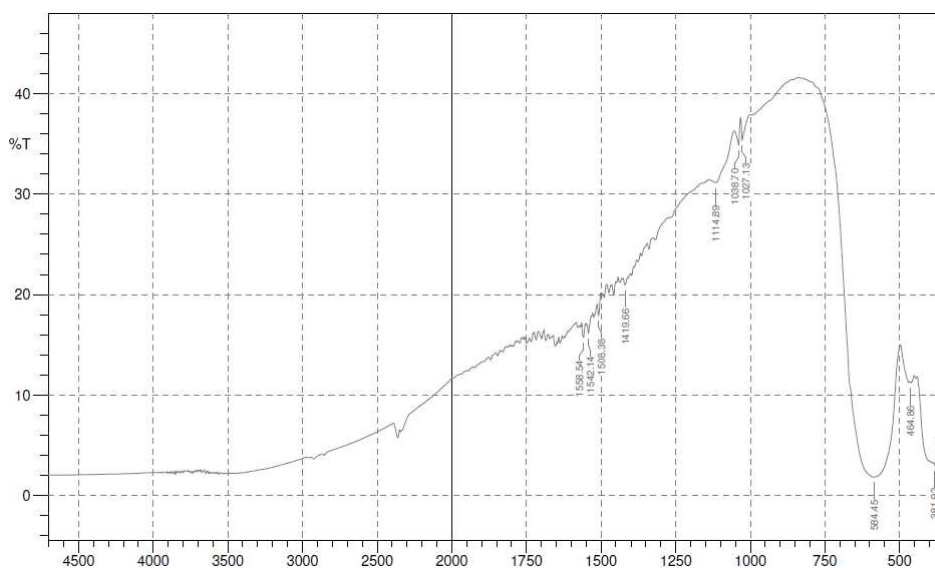


Figure 1: FTIR spectrum for  $\text{Ni}_{1-x}\text{Co}_x\text{Fe}_2\text{O}_4$  ( $X=0.3$ )

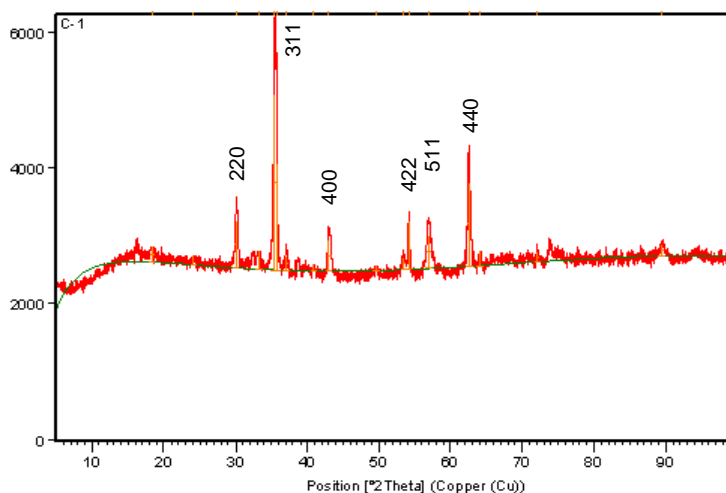


Figure 2: X-ray diffraction pattern for  $\text{NiFe}_2\text{O}_4$

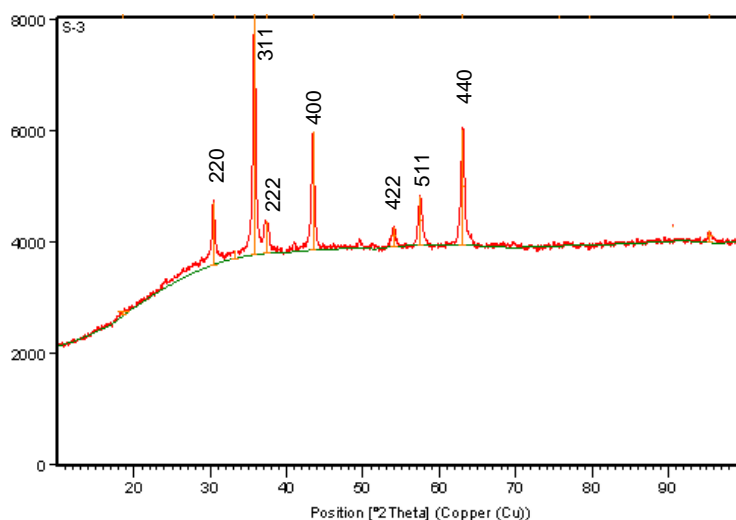


Figure 3: X-ray diffraction pattern for  $\text{Ni}_{1-x}\text{Co}_x\text{Fe}_2\text{O}_4$  ( $X=0.3$ )

X-ray diffraction studies (XRD) (figure 2, 3) show the formation of single phase spinel ferrites. No extra peaks (due to secondary phase) have been observed. XRD studies also verify increase in lattice parameter with cobalt substitution, which is due to replacement of smaller  $\text{Ni}^{2+}$  ions (0.069 nm) by larger  $\text{Co}^{2+}$  ions (0.074 nm) as per Vegard's law [20]. Average crystallite size of ferrite samples is calculated as 17-28 nm from X-ray diffraction studies (by using Scherrer equation) [31]. Particle size of synthesized ferrite samples also increases with cobalt substitution as atomic radius of cobalt is more than nickel.

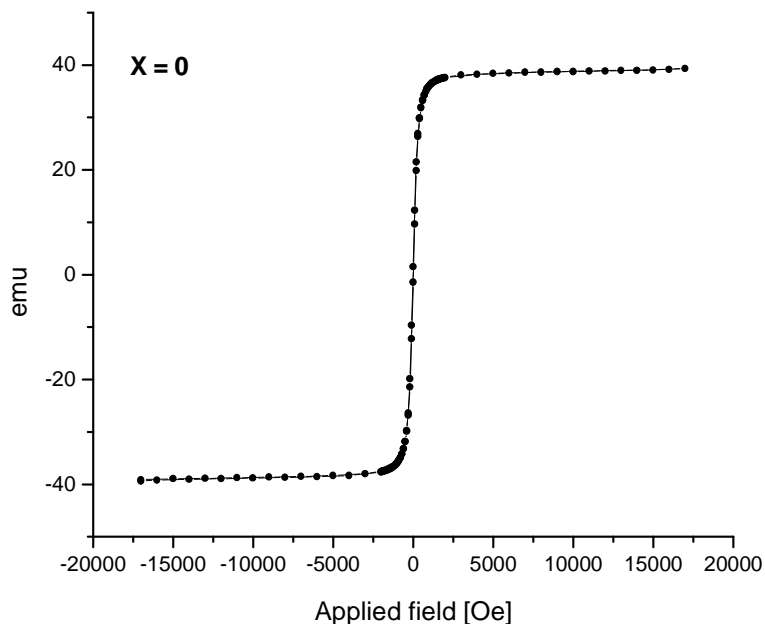
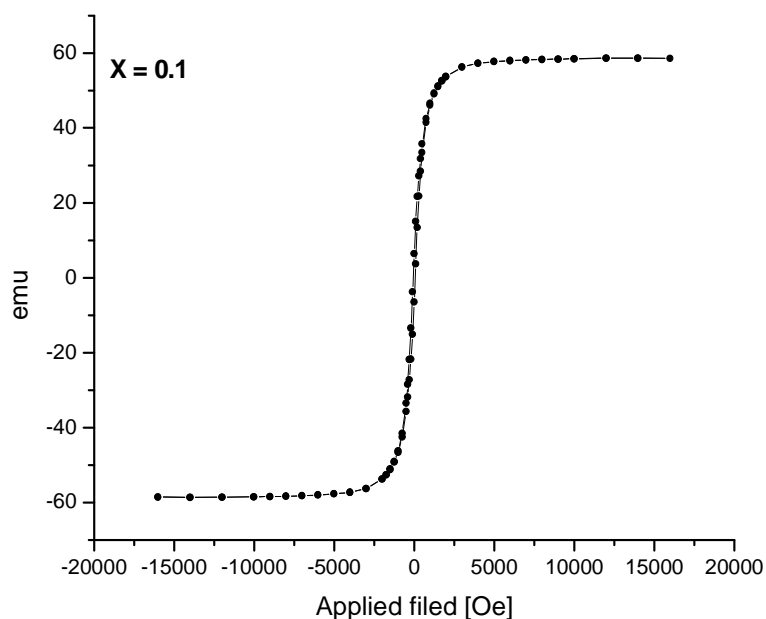
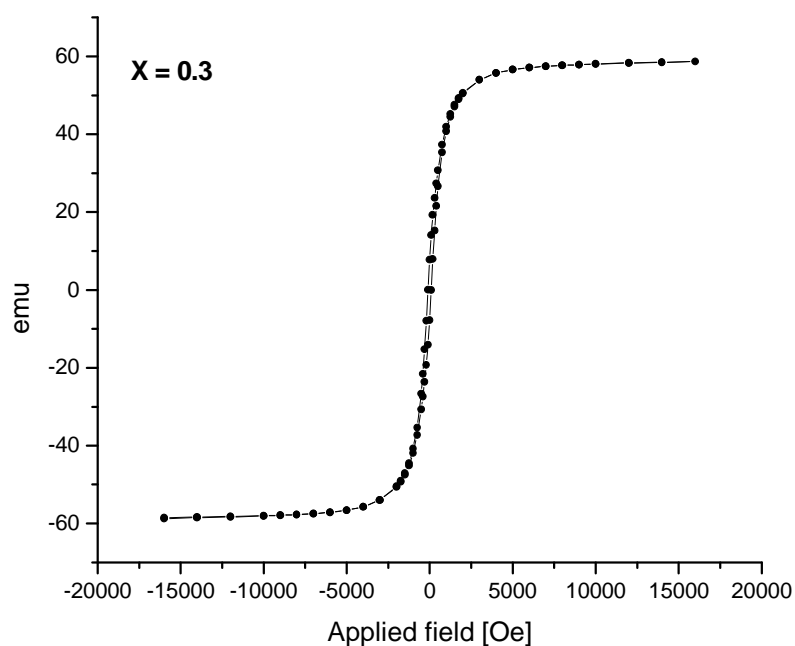
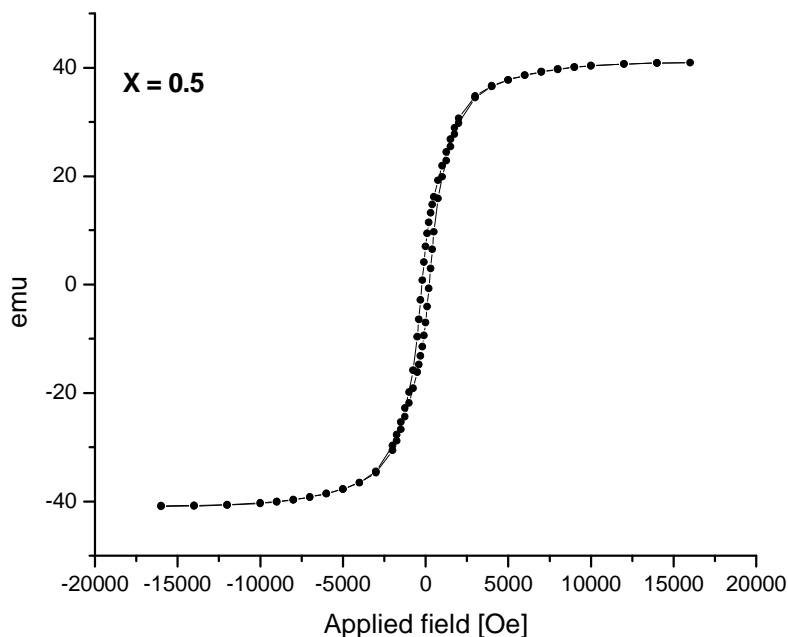


Figure 4: Hysteresis loop for  $\text{NiFe}_2\text{O}_4$

Figure 5: Hysteresis loop for  $\text{Ni}_{1-x}\text{Co}_x\text{Fe}_2\text{O}_4$ Figure 6: Hysteresis loop for  $\text{Ni}_{1-x}\text{Co}_x\text{Fe}_2\text{O}_4$ 

Figures 4-7 show hysteresis loop properties of ferrite samples. Magnetic parameters for  $\text{Ni}_{1-x}\text{Co}_x\text{Fe}_2\text{O}_4$  recorded at room temperature are listed in Table 1. With increase in cobalt content in the ferrite sample the value of coercive field is also increasing which could be attributed to larger magneto crystalline anisotropy constant of  $\text{Co}^{2+}$ , with respect to that of  $\text{Ni}^{2+}$  ions. The saturation magnetization increases up to  $x=0.3$  and then decreases. The increase in saturation magnetization is due to substitution of  $\text{Co}^{2+}$  ions, which have high magnetic moment in comparison to  $\text{Ni}^{2+}$  ions. However, decrease in saturation magnetization for  $x=0.5$  may be due to the fact that the magnetic spins of ions in neighboring A (tetrahedral) and B sites (octahedral) are anti-ferromagnetically coupled.

Figure 7: Hysteresis loop for  $\text{Ni}_{1-x}\text{Co}_x\text{Fe}_2\text{O}_4$ Table 1: Magnetic parameters for  $\text{Ni}_{1-x}\text{Co}_x\text{Fe}_2\text{O}_4$  recorded at room temperature

Sample	Coercive field (Oe)	Saturation magnetization (emu)
x=0	13.24	39.35
x=0.1	63.27	58.63
x=0.3	100.42	58.70
x=0.5	220.20	40.92

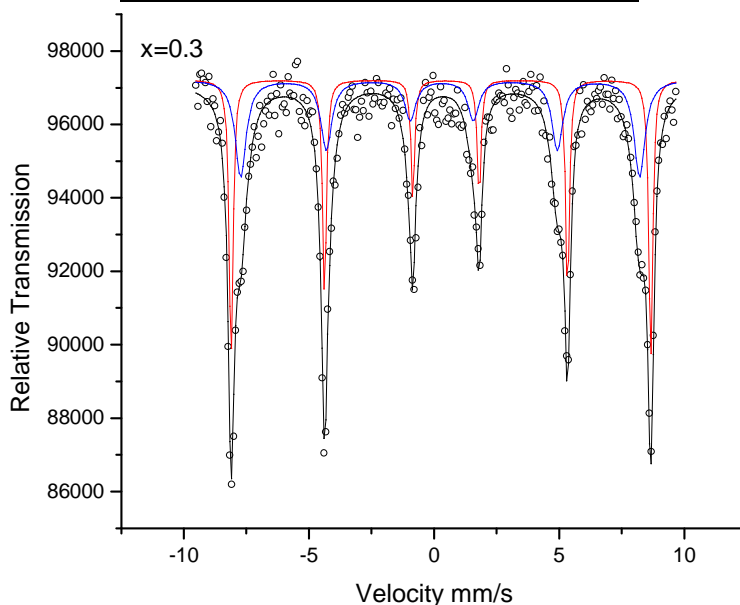
Figure 8: Mossbauer spectrum for  $\text{Ni}_{1-x}\text{Co}_x\text{Fe}_2\text{O}_4$ , (x=0.3)

Figure 8 shows room temperature Mössbauer spectrum of  $\text{Ni}_{1-x}\text{Co}_x\text{Fe}_2\text{O}_4$  (x=0.3). Two well resolved Zeeman sextets are seen which reveals ferrimagnetic nature of the ferrite composition. These sextets arise due to distribution of  $\text{Fe}^{3+}$  ions in both tetrahedral (A) and octahedral (B) sites [32]. The isomer shift values are  $0.28 \text{ mms}^{-1}$  and  $0.37$

$\text{mms}^{-1}$  respectively for A and B sites. Quadrupole splitting and internal magnetic field (magnetic hyperfine field) values for A site are  $0.002 \text{ mms}^{-1}$  and 49.42 Tesla, while for B site are  $0.004 \text{ mms}^{-1}$  and 51.98 Tesla.  $\text{Fe}^{3+}$  ions distribution for A and B sites are 48.992% and 51.002% respectively.

### CONCLUSION

Cobalt substituted nickel ferrites,  $\text{Ni}_{1-x}\text{Co}_x\text{Fe}_2\text{O}_4$ , have been synthesized by using oxalic dihydrazide as a fuel. Nano-scale ferrite particles can be synthesized by using solution combustion method. As the combustion process involves exothermic reaction and a large amount of heat is released, the ferrites can be synthesized at lower temperature. X-ray diffraction studies reveal the formation of single phase spinel structure. Magnetic studies show variation of coercivity and saturation magnetization with cobalt substitution and show higher coercivity and saturation magnetization than pure nickel ferrites. From the Mössbauer recording, presence of two well resolved Zeeman sextets, which is due to  $\text{Fe}^{3+}$  ions distribution in tetrahedral and octahedral sites, ferrimagnetic nature of ferrite materials is revealed.

### Acknowledgement

Authors are thankful to Guru Nanak Dev University, Amritsar, Punjab for X-ray diffraction, Mössbauer and Magnetic studies.

### REFERENCES

- [1] JL Xie; M Han; L Chen; R Kuang; L Deng. *J. Magn. Magn. Mater.*, **2007**, 314(1), 37–42.
- [2] P Mathur; A Thakur; JH Lee; M Singh. *Mater. Lett.*, **2010**, 64(24), 2738–2741.
- [3] S Xiang; W Yan-Xin; Y Xiang; X Yong; Z Jian-Feng, T Pie-Duo. *T. Nonferr. Met. Soc.*, **2009**, 19(6), 1588–1592.
- [4] AS Albaguerye; JD Ardisson; WAA Macedo; MCM Alves. *J. Appl. Phys.*, **2000**, 87(9), 4352.
- [5] A Goldman. *Modern Ferrite Technology*, Van Nostrand Reinhold, New York, **1990**.
- [6] V Blasko; V Petkov; V Rusanov; LIM Martinez; B Martinez; JS Munoz; M Mikhov. *J. Magn. Magn. Mater.*, **1996**, 162(2-3), 331-337.
- [7] O Caltun; H Chiriac; N Lupu; I Dumitru; BA Rao. *J. Optoelectro. Adv. Mater.*, **2007**, 9(4), 1158-1160.
- [8] NN Greenwood; TC Gibb. *Mössbauer Spectroscopy*, Chapman and Hall Ltd., London, **1971**.
- [9] S Nasir; M Anis-Ur-Rehman. *Phys. Scr.*, **2011**, 84(4), 025603–025609.
- [10] IH Gul; W Ahmed; A Maqsood. *J. Magn. Magn. Mater.*, **2008**, 320(3-4), 270-275.
- [11] S Zahi; M Hashim; AR Daud. *J. Magn. Magn. Mater.*, **2007**, 308(2), 177–182.
- [12] N Singh; A Agarwal; S Sanghi; P Singh. *Physica B.*, **2011**, 406(3), 687-692.
- [13] X Li; G Wang. *J. Magn. Magn. Mater.*, **2009**, 321(9), 1276-1279.
- [14] A Verma; TC Goel; RG Mendiritta; P Kishan. *J. Magn. Magn. Mater.*, **2000**, 208(1-2), 13-19.
- [15] PP Sarangi; SR Vadera; MK Patra; NN Ghosh. *Powder Technol.*, **2010**, 203(2), 348-353.
- [16] AS Prakash; AMA Khadar; KC Patil; MS Hegde. *J. Magn. Magn. Mater.*, **2002**, 10(3), 135-141.
- [17] P Priyadharsini; A Pradeep; G Chandrasekaran. *J. Magn. Magn. Mater.*, **2009**, 321(12), 1898-1903.
- [18] MM Mallapur; BK Chougule. *Mater. Lett.*, **2010**, 64(3), 231-234.
- [19] A Ghasemi; AP Jr; CFC Machado. *J. Magn. Magn. Mater.*, **2012**, 324(14), 2193-2198.
- [20] M Mozaffari; J Amighian; E Darsheshdar. *J. Magn. Magn. Mater.*, **2014**, 350(1), 19-22.
- [21] AS Fawzi; VL Mathe; AD Sheikh. *Physica B.*, **2010**, 405(91), 340-344.
- [22] A Khan; PG Smirniotis. *J. Mol. Catal. A-Chem.*, **2008**, 280(1-2), 43–51.
- [23] K Mukherjee; SB Majumder. *Nanotechnology*, **2010**, 21(25):255504–255509.
- [24] UB Gawas; VMS Verenkar; DR Patil. *Sens. Trans.*, **2011**, 134, 45–55.
- [25] QA Pankhurst; J Connolly; SK Jones; J Dobson. *J. Phys. D: Appl. Phys.*, **2003**, 36(13), 167-181.
- [26] D Gherca; C Virlan; RG Ciocarlan; T Toman; N Cornei; A Pui. *Acta Chem. IASI*, **2013** 21, 19-30.
- [27] NM Mahmoodi. *Desalination*, **2011**, 279(1-3), 332–337.
- [28] MM Niyaz; SG Sajjid; SK Moosa. *Environ. Monit. Assess.*, **2013**, 185(12), 10235-10248.
- [29] Y Koseoglu; M Bay; M Tan; A Baykal; H Sozeri; R Topkaya; N Akdogan. *J. Nanopart. Res.*, **2011**, 13(5), 2235–2244.
- [30] RDD Waldron. *Phys. Rev.*, **1955**, 99, 1727–1735.
- [31] BD Cullity. *Elements of X-Ray Diffraction*, Addison Wesley Co., **1978**.
- [32] GJ Long. *Mössbauer Spectroscopy Applied to Inorganic Chemistry Volume 2*, Plenum Press, New York, **1989**.